# Laser Scanning for Single-Shot Frequency Diverse Photoacoustic Excitation

William L. Meng, Aidan Fitzpatrick, Ajay Singhvi, and Amin Arbabian
Department of Electrical Engineering, Stanford University, Stanford, CA, USA

***Abstract*—Photoacoustic and laser-induced ultrasound based imaging systems have been successfully deployed for a range of applications from biomedical imaging to non-destructive testing and remote sensing. Application-specific optimization of the spatial, spectral, and temporal properties of the generated photoacoustic waves requires careful consideration of the optical excitation sub-system. In this work, we study, both analytically and through simulations, the effects of a moving laser source on the generated photoacoustic waves and discuss the additional degrees-of-freedom provided by scanning the laser in a laser-induced ultrasound imaging system. By tuning laser parameters such as the laser scan velocity and modulation frequency, we explore the utility of a moving laser in implementing transmit beam-steering as well as in the generation of angle-dependent, multi-frequency acoustic waves. Finally, as an example application, we demonstrate single-shot, single-sensor imaging.**

***Index Terms*—beam-steering, Doppler, k-Wave, laser scanning, laser ultrasound, multi-frequency, photoacoustics, single sensor**

## I. Introduction

Laser-induced ultrasound (LUS) based imaging systems that leverage the photoacoustic (PA) effect have been successfully deployed for a range of sensing applications. The multi-modal nature of the system provides a means for remote generation of ultrasonic (US) waves while maintaining the advantages of good mechanical contrast and high US resolution. This includes biomedical applications such as medical imaging and elastography [1], [2], non-destructive testing applications such as material characterization, fault detection, and thickness estimation [3] as well as remote cross-medium sensing [4], [5].

Through the decoupling of excitation and detection sub-systems, LUS sensing provides many design knobs that can be used to tailor the system towards a particular application. There is much ongoing research tackling the problem of more efficient and deeper laser excitation, along with high resolution, array-based optical or US detection methods [6] to enable increasingly complex and challenging applications. However, while the research and development of LUS systems has been ongoing for decades [3], most such systems currently deploy a stationary laser source [1]–[4] that radiates a roughly isotropic acoustic wave such that the acoustic spectrum is the same in every direction, as illustrated conceptually in Fig. 1(a).

In this work, we utilize the degrees-of-freedom afforded by the laser excitation sub-system by leveraging the fact that a moving laser source radiates spatially varying acoustic spectra in each direction. As conceptually shown in Fig. 1(b), a moving laser source generates different Doppler shifts depending upon the direction of observation. In the following sections, we analyze, via theory and end-to-end LUS simulations, the advantages that can be gained by varying laser speeds, laser modulation schemes, and ultrasonic detection parameters to enable novel iterations of next-generation LUS systems.

This material is based upon work supported by the National Science Foundation Graduate Research Fellowship Program under Grant No. DGE-1656518.

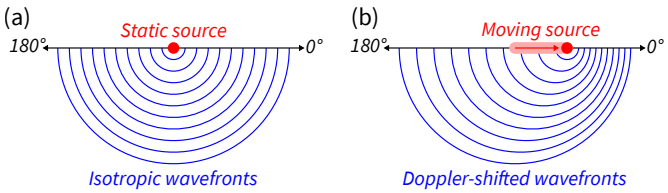


Fig. 1. (a) Isotropic acoustic wavefronts generated by a static laser excitation source and (b) Doppler-shifted acoustic wavefronts generated by a moving laser source.

Specifically, as schematically shown in Fig. 2, we will focus on two iterations of a moving LUS system. Firstly, by varying the laser scanning speed and modulation frequency, transmit beam-steering of an individual temporal acoustic frequency component can be achieved. Secondly, a scanning laser excites spatially selective acoustic waves across a range of frequencies, improving target localization by encoding each spatial angle with a different temporal frequency. Finally, we demonstrate an example implementation of a LUS imaging system, wherein by leveraging the advantages afforded by a moving laser source, one can obtain images of the sample using a single sensor in a single shot, which has numerous use-cases in resource-constrained applications.

## II. Background

Upon laser irradiation, optical absorbers are subjected to a rapid temperature rise that results in thermal expansion. At the boundaries of differential thermal expansion, pressure waves are generated and subsequently propagate radially outward [7]. As previously mentioned, this physical phenomenon has a number of applications in PA and LUS sensing and imaging.

Conventional LUS employs a static laser focal point for the duration of the excitation, which generates PA signals that are proportional to the laser modulation function [8]:

$$P(f) \propto f \cdot H(f), \tag{1}$$

where $P$ is the generated acoustic pressure, $H$ is the laser intensity modulation function, and $f$ is the temporal frequency. Through this proportionality, the temporal frequency components within the laser modulation function translate to the spectrum of the generated acoustic pressure.

2022 IEEE International Ultrasonics Symposium (IUS) | 978-1-6654-6657-8/22/$31.00 ©2022 IEEE | DOI: 10.1109/IUS54386.2022.9957210

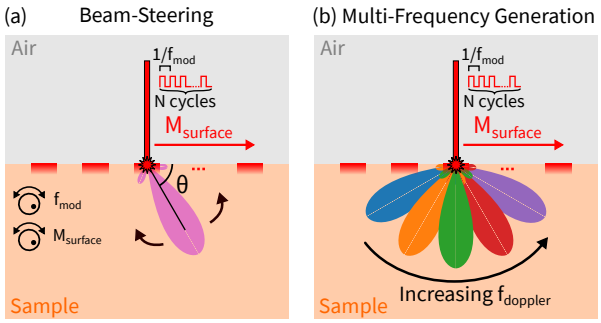


Fig. 2. Conceptual diagram for using the proposed scanning laser ultrasound system for (a) transmit beam-steering and (b) spatially selective, multi-frequency photoacoustic excitation

However, when the laser is instead scanned over the sample at an appreciable fraction of the speed of sound, given by the Mach number $M_{\text{surface}}$, the generated acoustic pressure incurs an angle-dependent Doppler shift, as shown in Fig. 1(b), thus resulting in a spatially varying acoustic spectrum [9]:

$$P(f,\theta) \propto f \cdot H\left(\frac{f}{1-M(\theta)}\right), \tag{2}$$

where $M(\theta)$ is the velocity component of $M_{\text{surface}}$ at the observer's angle $\theta$, measured from the plane of the laser scan:

$$M(\theta) = M_{\text{surface}} \cos\theta. \tag{3}$$

In the remainder of this paper, we explore the advantages and potential applications of the angle-dependent Doppler shift resulting from a scanned laser ultrasonic excitation.

While the results presented in this paper are simulation-based, it is important to note how practical implementation could constrain feasible laser scan velocities. Through the use of a low-mass, rotating mirror (whose angle is controlled by a mechanical actuator) combined with a sufficiently large standoff distance, $M_{\text{surface}} \leq 1$ can be feasibly achieved with minimal physical motion, as demonstrated in other works [9]. Lastly, while the US frequencies investigated in this work were chosen based on prior work [4], the ideas presented throughout the paper are broadly applicable across a range of sensor configurations depending upon application requirements.

## III. Transmit Beam-Steering

Conventional approaches for steering an acoustic beam transmitted by a physical transducer typically fall into one of two categories: (1) mechanical steering of a single, fixed-focused transducer, or (2) electronic beam-steering using a phased array. These are both interference-based approaches to beam-steering, which use constructive interference to enhance the energy within the beam, and destructive interference to suppress energy outside the beam [10].

Unfortunately, neither of these approaches lends itself well to LUS imaging systems. Since the laser-induced acoustic source is not a physical transducer, it cannot be rotated mechanically. In addition, while the acoustic beamwidth can be controlled via the laser spot size [4], it is more challenging to control the beam's propagation direction via electronic beam-steering. One approach could be to create a laser-induced acoustic phased array using a large number of independently modulated lasers, though this would greatly increase system cost and complexity.

In this section, we present an approach that uses a single moving laser for optically controlled steering of a narrowband acoustic beam that is captured by a matched narrowband acoustic sensor. First, the laser intensity is modulated with a modulation frequency $f_{\text{mod}}$ and produces a narrowband acoustic source upon absorption by the sample as shown in equation (1). Without moving the laser, this acoustic pressure would propagate in all directions without any change in wavelength, thus the transmit beam pattern would be isotropic and the acoustic frequency of the wavefronts would be equal to $f_{\text{mod}}$ in all directions. In such a case, $f_{\text{mod}}$ would be chosen to match the narrowband sensor frequency $f_{\text{sensor}}$.

On the other hand, when the laser is moved with a constant velocity $M_{\text{surface}}$, the acoustic wavefronts experience an angle-dependent Doppler shift, with the Doppler-shifted frequency $f_{\text{doppler}}$ given by:

$$f_{\text{doppler}} = \frac{f_{\text{mod}}}{1 - M_{\text{surface}} \cos\theta}. \tag{4}$$

Thus, by appropriately varying the modulation frequency $f_{\text{mod}}$ and/or the laser scan velocity $M_{\text{surface}}$, we can steer the transmit beam such that $f_{\text{doppler}}$ matches the sensor frequency $f_{\text{sensor}}$ at the desired beam-steering angle $\theta$.

In order to validate the above theory, we used the MATLAB k-Wave [11] simulation toolbox to run end-to-end scanning LUS simulations. The simulation setup used to characterize the transmit beam pattern of the generated acoustic waves is shown in Fig. 3(a). A moving PA source was placed in the center of the simulated air-sample interface and a semi-circular array of narrowband sensors, with center frequency $f_{\text{sensor}} = 71\ kHz$ and bandwidth $1\ kHz$, were placed in the far-field to map the directivity patterns; the sample was assumed to be water.

Assuming a fixed $M_{\text{surface}}$, we can determine the $f_{\text{mod}}$ required to tune $\theta$ for the specified $f_{\text{sensor}}$ using the design equation below:

$$f_{\text{mod}} = f_{\text{sensor}}\left(1 - M_{\text{surface}} \cos\theta\right). \tag{5}$$

The resulting directivity plot in Fig. 3(b) obtained from the LUS simulations, with a fixed $M_{\text{surface}} = 0.5$, shows that by modifying $f_{\text{mod}}$ from approximately 40 $kHz$ to 100 $kHz$, we are able to steer the 71 $kHz$ beam from roughly 30° to 150° as expected from the above equation.

One can also vary $M_{\text{surface}}$ to steer the acoustic beam, provided $f_{\text{mod}}$ is chosen such that it differs from $f_{\text{sensor}}$. The laser scan velocity is then given by:

$$M_{\text{surface}} = \frac{1 - f_{\text{mod}}/f_{\text{sensor}}}{\cos\theta}. \tag{6}$$

LUS simulations validate the above equation, with the obtained directivity plot in Fig. 3(c) demonstrating beam-steering of the 71 $kHz$ beam from roughly 30° to 150° by

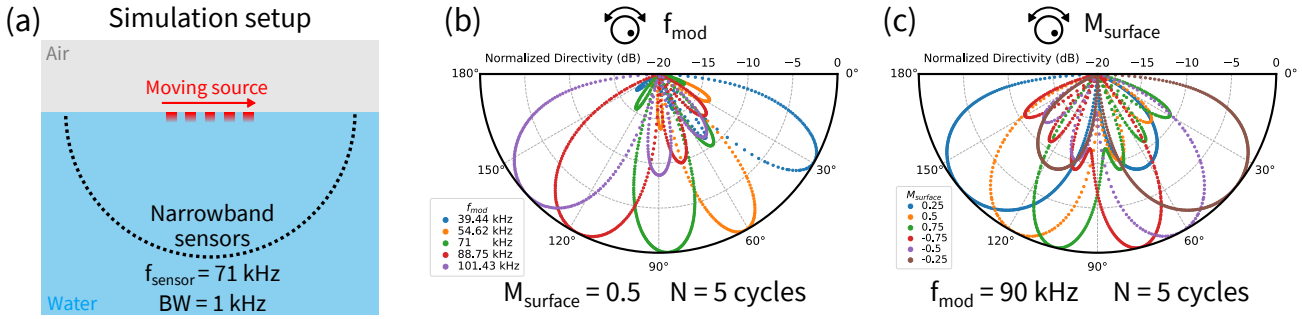


Fig. 3. (a) Simulation setup for characterizing the transmit beam steering pattern, with results shown for tuning (b) $f_{\text{mod}}$ or (c) $M_{\text{surface}}$.

varying $M_{\text{surface}}$ from -0.75 to 0.75, with $f_{\text{mod}}$ = 90 $kHz$. Note that it is impossible to achieve $\theta = 90°$ by tuning only $M_{\text{surface}}$ because the required scan velocity approaches impractically high values. Thus, $f_{\text{mod}}$ is a more suitable tuning knob for applications which require steering at these angles.

Therefore, depending upon system constraints, using our proposed laser scanning approach the angle of a beam can be steered by adjusting the modulation frequency $f_{\text{mod}}$ and/or the scanning velocity $M_{\text{surface}}$.

## IV. Multi-Frequency Generation

In the previous section, we assume the use of a narrowband sensor that spatially samples only the angular span at which the Doppler-shifted frequency matches the sensor frequency. However, if we instead use a broadband sensor, we could capture more of the Doppler-shifted spectrum to simultaneously sample a larger angular span. Unlike conventional broadband LUS systems, the proposed scanning LUS system has spatial information encoded in the temporal frequency components due to the angle-dependent Doppler shift. As will be discussed in the remainder of this section, this precise angle-to-frequency mapping can be leveraged for enhanced multi-frequency sensing.

### A. Angle-To-Frequency Mapping

From equation (4), there is a one-to-one mapping between $\theta$ and $f_{\text{doppler}}$ when $0 < M_{\text{surface}} < 1$. Under this condition, the angle of an arbitrary point in space can be uniquely determined from the value of $f_{\text{doppler}}$ seen at the point using:

$$\theta = \cos^{-1}\left(\frac{1 - f_{\text{mod}}/f_{\text{doppler}}}{M_{\text{surface}}}\right). \tag{7}$$

In order to detect the entire span of angles $\theta \in [0, 180]$, $f_{\text{mod}}$ and $M_{\text{surface}}$ should be chosen such that the span of Doppler-shifted frequencies

$$f_{\text{doppler}} \in \left[\frac{f_{\text{mod}}}{1 + M_{\text{surface}}}, \frac{f_{\text{mod}}}{1 - M_{\text{surface}}}\right]$$

falls within the sensor's bandwidth.

A LUS simulation was conducted in k-Wave to verify the above angle-to-frequency mapping scheme, with the simulation setup shown in Fig. 4(a). Fig. 4(b) shows a directivity plot with a subset of simultaneously generated angle-dependent Doppler-shifted frequencies varying from approximately 50 $kHz$ to 130 $kHz$ over a 30° to 150° angular span.

### B. Single-Shot, Single-Sensor Imaging

In conventional imaging systems, a single sensor can only capture 1D spatial information in which range is encoded in time. By utilizing an array of sensors, an additional axis of spatial information can be captured to enable 2D imaging. However, in certain resource-constrained or challenging sensing scenarios, employing a large sensor array is impractical due to its added complexity, cost, and computational intensiveness. Instead, the angle-to-frequency mapping discussed earlier could be used to perform single-shot, 2D imaging using a single sensor by encoding range information into the signal's time axis and angular information into the signal's frequency axis.

To demonstrate the proposed single-shot, single-sensor imaging we again utilize the MATLAB k-Wave [11] simulation toolbox, with the setup shown in Fig. 4(a). As the laser is scanned across the sample, the Doppler-shifted acoustic spectrum is generated. While propagating through the sample, the acoustic waves are backscattered by a number of point targets and the reflected signals are captured by a single broadband sensor located at the surface of the sample. The reflected signal from each point target has the same frequency as the Doppler-shifted wave incident on the target, and thus the frequency of each echo encodes the angular position of each target, while the time-of-arrival of the echo encodes the range of the target.

The 2D locations of the point targets can be recovered from the 1D sensor data using the algorithm illustrated in Fig. 4(c). First, Time Gain Compensation (TGC) is applied to the raw sensor data to account for spreading loss due to propagation of the acoustic waves, and a bandpass filter is applied to remove frequencies outside of the sensor bandwidth. The resulting time-domain signal is then fed into a bank of matched filters defined over discrete frequencies within the sensor bandwidth to yield a representation of the frequency content at each time. The time and frequency axes are then mapped to range and angle axes through the below relationship:

$$(r, \theta) = \left(\frac{tc_{\text{sample}}}{2}, \cos^{-1}\left(\frac{1 - f_{\text{mod}}/f}{M_{\text{surface}}}\right)\right), \tag{8}$$

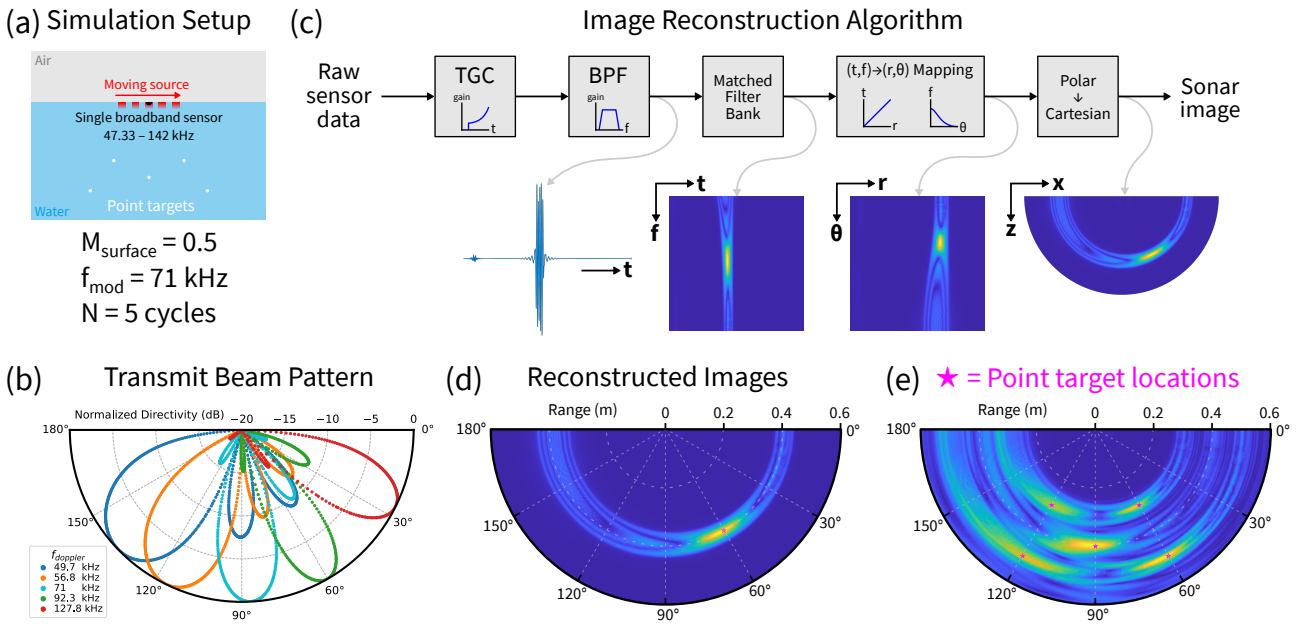


Fig. 4. (a) Simulation setup, (b) transmit beam pattern, and (c) reconstruction algorithm for single-shot, single sensor 2D sonar imaging. Reconstructed images are shown for (d) 1 point target and (e) 5 point targets.

where $c_{\text{sample}}$ is the speed-of-sound in the simulated sample medium. Lastly, polar coordinates are converted to Cartesian coordinates to yield the final 2D image.

In Fig. 4(d), we show the reconstructed image of a single point target that matches well with the expected range and angle, validating the reconstruction pipeline discussed above. Next, we show a reconstructed image of five point targets, placed such that multiple targets appear at the same range away from the sensor. Normally, with a single 1D signal captured by a single-sensor, targets at the same range would be indistinguishable due to overlapping echoes in the time-domain. However, by also leveraging spectral information provided by the proposed single-shot scanning LUS system, we are able to accurately reconstruct the multiple targets. As shown in Fig. 4(e), the reconstructed target ranges and angles match well with the ground-truth.

In applications where real-time single-shot imaging is not required, additional configurations of $f_{\text{mod}}$ and $M_{\text{surface}}$ could be used sequentially to further improve performance. In addition, this approach could be employed with an array of broadband sensors to combine the benefits of spatial, spectral, and temporal diversity.

## V. Conclusion

In this paper, we propose design techniques for laser ultrasound imaging systems that incorporate a moving laser rather than a static one, leveraging the Doppler shift created by the laser scanning to add additional degrees-of-freedom for system design. Firstly, the laser-induced acoustic beam can be steered by adjusting the modulation frequency and scanning velocity of the laser. Secondly, the spatially-varying, frequency-diverse acoustic field produced by laser scanning creates a one-to-one mapping between angle and frequency which encodes two-dimensional spatial information into one-dimensional signals. Such a design concept can be used for applications such as single-shot, two-dimensional imaging with a single sensor among others.

## References


[1] X. Zhang *et al.*, "Full noncontact laser ultrasound: first human data," *Light: Science & Applications*, vol. 8, no. 1, pp. 1–11, 2019.

[2] J. L. Johnson, J. Shragge, and K. Van Wijk, "Nonconfocal all-optical laser-ultrasound and photoacoustic imaging system for angle-dependent deep tissue imaging," *Journal of Biomedical Optics*, vol. 22, no. 4, p. 041014, 2017.

[3] S. Davies *et al.*, "Laser-generated ultrasound: its properties, mechanisms and multifarious applications," *Journal of Physics D: Applied Physics*, vol. 26, no. 3, p. 329, 1993.

[4] A. Fitzpatrick, A. Singhvi, and A. Arbabian, "An Airborne Sonar System for Underwater Remote Sensing and Imaging," *IEEE Access*, vol. 8, pp. 189 945–189 959, 2020.

[5] A. Singhvi, A. Fitzpatrick, and A. Arbabian, "An Electronically Tunable Multi-Frequency Air-Coupled CMUT Receiver Array with sub-100$\mu$Pa Minimum Detectable Pressure Achieving a 28kb/s Wireless Uplink Across a Water-Air Interface," in *2022 IEEE International Solid-State Circuits Conference (ISSCC)*, vol. 65. IEEE, 2022, pp. 498–500.

[6] F. Gao, X. Feng, and Y. Zheng, "Advanced photoacoustic and thermoacoustic sensing and imaging beyond pulsed absorption contrast," *Journal of Optics*, vol. 18, no. 7, p. 074006, 2016.

[7] Wang, Lihong V. and Wu, Hsin-i, *Biomedical Optics: Principles and Imaging*. John Wiley & Sons, Ltd, 2007, ch. 12, pp. 283–321.

[8] F. Blackmon, L. Estes, and G. Fain, "Linear optoacoustic underwater communication," *Applied Optics*, vol. 44, no. 18, pp. 3833–3845, 2005.

[9] N. P. Chotiros, "The moving thermoacoustic array: A theoretical study," *The Journal of the Acoustical Society of America*, vol. 83, no. 6, pp. 2145–2158, 1988.

[10] O. T. Von Ramm and S. W. Smith, "Beam Steering with Linear Arrays," *IEEE Transactions on Biomedical Engineering*, vol. BME-30, no. 8, pp. 438–452, 1983.

[11] Treeby, B. E. and Cox, B. T., "k-Wave: MATLAB toolbox for the simulation and reconstruction of photoacoustic wave-fields," *Journal of Biomedical Optics*, vol. 15, no. 2, p. 021314, 2010.